

Cationic rhodium(III) bisdimethylglyoximates with water and triphenylphosphine axial ligands

Monika Moszner ^{a,*}, Fioretta Asaro ^b, Silvano Geremia ^b, Giorgio Pellizer ^b,
Claudio Tavagnacco ^b

^a Faculty of Chemistry University of Wrocław, 14 F. Joliot-Curie Street, 50383 Wrocław, Poland

^b Dipartimento di Scienze Chimiche, Università degli Studi di Trieste, Via Giorgieri 1, 34127 Trieste, Italy

Received 17 September 1996; revised 4 November 1996; accepted 25 November 1996

Abstract

Preparations of $[\text{Rh}(\text{Hdmg})_2(\text{H}_2\text{O})_2]\text{ClO}_4$ (**1**) (Hdmg = dimethylglyoximate) from $[\text{Rh}(\text{H}_2\text{O})_6](\text{ClO}_4)_3$ and dimethylglyoxime and of $[\text{Rh}(\text{Hdmg})_2(\text{PPh}_3)_2]\text{ClO}_4$ (**2**) from **1** and PPh_3 are described. **1** crystallizes in the $C2/c$ space group with $a = 14.910(3)$, $b = 6.058(1)$, $c = 18.617(4)$ Å, $\beta = 107.649(8)^\circ$, $Z = 4$. The structure was refined up to $R = 0.021$ for 1849 reflections. The IR and NMR spectra and electrochemical behavior of **1** and **2** are discussed and compared with other rhodoximes. Three polarographic and CV processes can be detected for **2**, the first two, respectively to Rh(II) and Rh(I), being followed by fast reactions.

Keywords: Rhodium complexes; Oxime complexes; Electrochemistry; Crystal structures

1. Introduction

Rhodium complexes with the tetradentate bisdimethylglyoximate, $(\text{Hdmg})_2$, equatorial ligand (rhodoximes) are receiving considerable attention [1]. Besides showing very promising catalytic properties in hydrogenation and hydrosilylation reactions [2], they are contributing to a better understanding of metal bisdimethylglyoximate complexes, especially of cobaloximes, well known useful models of vitamin B_{12} molecules [3].

A good number of six-coordinate rhodoximes $[\text{Rh}(\text{Hdmg})_2\text{LX}]$ have been synthesized and studied [4], but their behavior, especially the electrochemical aspects [5], has not been investigated to the same extent as that of cobaloximes yet. Important advances were made in the explanation of the role of the electronic and steric properties of the axial alkyls in organorhodoximes [1], but little attention was paid to other axial ligands. The study of $[\text{Rh}(\text{Hdmg})_2\text{L}_2]$ derivatives, with higher symmetry and with equatorial arrangement nearer to planarity, is expected to widen the knowledge of the effects of the axial ligands. Among them the $[\text{Rh}(\text{Hdmg})_2(\text{H}_2\text{dmg})\text{Cl}_2]$ [6], $[\text{Rh}(\text{Hdmg})_2\text{Cl}_2]^-$ [7], $[\text{Rh}(\text{Hdmg})(\text{dmg})\text{Cl}_2]^{2-}$ [8], $[\text{Rh}(\text{Hdmg})_2(\text{L})_2]^+$ (L = nitrogen base) [9] and $[\text{Rh}(\text{Hdmg})_2(\text{PPh}_3)_2]^+$ [4g] species have already been reported.

Here we describe the synthesis, the isolation, the IR and NMR spectra of the $[\text{Rh}(\text{Hdmg})_2(\text{H}_2\text{O})_2]\text{ClO}_4$ and $[\text{Rh}(\text{Hdmg})_2(\text{PPh}_3)_2]\text{ClO}_4$ compounds, the X-ray structure of the former and some electrochemical properties of the latter.

2. Experimental

2.1. Spectroscopic measurements

UV–Vis: room temperature spectra were monitored in the 200–820 nm range by a Perkin–Elmer Lambda 5 and a Hewlett Packard 8452A rapid scan diode array spectrometer.

IR: the spectra were measured in the range $4000\text{--}400\text{ cm}^{-1}$ from KBr disks or Nujol mulls on a Perkin–Elmer 983G spectrometer.

NMR: the spectra were recorded on a JEOL EX-400 spectrometer (^1H at 400 MHz, ^{13}C at 100.5 MHz, ^{31}P at 161.7 MHz) and on a Bruker AMX-300 spectrometer (^1H at 300.1 MHz, ^{13}C at 75.5 MHz, ^{31}P at 121.5 MHz). For ^1H and ^{13}C spectra TMS was used as internal standard. For ^{31}P spectra 10% H_3PO_4 solution was used as external standard.

2.2. Materials

$\text{RhCl}_3 \cdot 3\text{H}_2\text{O}$ was purchased from Aldrich. All other chemicals were reagent grade and were used as commercially

* Corresponding author.

obtained. The compound $[\text{Rh}(\text{H}_2\text{O})_6](\text{ClO}_4)_3$ was synthesized according to the method of Ayres and Forrester [10] through the reaction of $\text{RhCl}_3 \cdot 3\text{H}_2\text{O}$ with concentrated perchloric acid. The solutions were standardized spectrophotometrically by the absorption spectrum of $[\text{Rh}(\text{H}_2\text{O})_6]^{3+}$ with bands at 311 ($\epsilon = 67.4 \text{ M}^{-1} \text{ cm}^{-1}$) and 396 ($\epsilon = 6.2 \text{ M}^{-1} \text{ cm}^{-1}$) nm [10].

Caution! Perchlorate salts of metal complexes are potentially explosive. Only a small amount of material should be prepared and handled with caution.

2.3. Electrochemistry

The measurements were made at $25 \pm 0.1^\circ\text{C}$ under Ar or N_2 in a three-electrode thermostated jacket cell. An Amel 552 potentiostat/galvanostat connected with an Amel 568 function generator was used for polarography. A home-made potentiostat [11], equipped with positive feedback and driven by a Hewlett Packard 3314A function generator, was used for fast cyclic voltammetry. A DME (dropping mercury electrode) was the working electrode for polarography and a Metrohm 663 VA Stand for Hg was used for cyclic voltammetry (CV). Concentrations of the investigated compounds in DMF were in the range between 2×10^{-4} and $1 \times 10^{-3} \text{ mol dm}^{-3}$; the supporting electrolyte was tetrabutylammonium perchlorate (TBAP).

2.4. Syntheses

2.4.1. $[\text{Rh}(\text{Hdmg})_2(\text{H}_2\text{O})_2]\text{ClO}_4(\text{I})$

(a) A solution of $[\text{Rh}(\text{H}_2\text{O})_6](\text{ClO}_4)_3$ (6 mmol) in HClO_4 (10–12 M) was cooled to $\sim 263 \text{ K}$ and concentrated aqueous KOH was added up to pH 2. After filtering off the precipitated KClO_4 and warming the yellow solution (bands at 311 and 396 nm), 1.42 g of dimethylglyoxime (H_2dmg 12.2 mmol), dissolved in hot ethanol (35 ml), were added. The reaction mixture, boiled for 45 min, turned dark orange (bands at 272 ($\epsilon = 9940 \text{ M}^{-1} \text{ cm}^{-1}$) and 340sh ($\epsilon = 2357 \text{ M}^{-1} \text{ cm}^{-1}$) nm). It was concentrated to $\sim 10 \text{ ml}$ and cooled overnight in a refrigerator. Further precipitation of KClO_4 occurred. The solution was filtered again, concentrated to 5 ml and left in the refrigerator until yellow crystals of **1** sep-

arated. These were washed quickly with a small amount of cool ethanol and next with ether and then dried in vacuo. Yield 30%.

(b) A solution of $[\text{Rh}(\text{H}_2\text{O})_6](\text{ClO}_4)_3$ (2 mmol) in concentrated (10–12 M) perchloric acid was diluted with H_2O up to 1 M HClO_4 . 0.48 g (4 mmol) H_2dmg , dissolved in 20 ml of hot ethanol, was added. The reaction mixture was boiled for 3 h, then concentrated to $\sim 2 \text{ ml}$, heating under vacuum, and left in a refrigerator until yellow crystals of compound **1** appeared. They were separated from the solution, quickly washed and dried as in (a). Yield 30%. *Anal.* Found: C, 20.7; H, 3.9; N, 11.7. *Calc.* for $\text{RhC}_8\text{H}_{18}\text{N}_4\text{O}_{10}\text{Cl}$: C, 20.5; H, 3.9; N, 11.9%. The compound is air stable, and soluble in water, methanol and ethanol.

2.4.2. $[\text{Rh}(\text{Hdmg})_2(\text{PPh}_3)_2]\text{ClO}_4(\text{2})$

10 ml ethanol and 1.1 g (4.1 mmol) of PPh_3 in 30 ml of hot ethanol were added to the concentrated mother liquor containing **1**, obtained as described in procedure (a). The mixture was boiled for 40 min. During the reaction the yellow solution turned orange-red with a strong absorption in the 450 nm region, possibly due to a dimeric Rh(II) species [12]. After filtering and standing, orange-yellow crystals separated. They were washed with ethanol, thoroughly with diethyl ether and dried under vacuum. Yield 60%. *Anal.* Found: C, 54.1; H, 4.7; N, 5.5. *Calc.* for $\text{RhC}_{44}\text{H}_{46}\text{N}_4\text{O}_9\text{P}_2\text{Cl}$: C, 54.2; H, 4.8; N, 5.7%.

2.5. X-ray analysis

Intensity data were collected on a CAD4 Enraf-Nonius single crystal diffractometer at room temperature by $\omega/2\theta$ scan technique using graphite-monochromated Mo $K\alpha$ radiation ($\lambda = 0.7107 \text{ \AA}$). Crystal data are reported in Table 1. The intensities were corrected for Lorentz and polarization factors. An empirical absorption correction, based on ψ scan, was applied. The structure was solved by conventional Patterson and Fourier methods and refined through full-matrix least-squares methods. The non-hydrogen atoms were treated anisotropically. The hydrogen atoms, located on positive regions of the $F_o - F_c$ Fourier map, were refined isotropically. A secondary extinction correction [13] was applied and the

Table 1
Crystal data for $[\text{Rh}(\text{Hdmg})_2(\text{H}_2\text{O})_2]\text{ClO}_4$

Formula	$\text{RhO}_6\text{N}_4\text{C}_8\text{H}_{18} \cdot \text{ClO}_4$	Crystal size (mm)	$0.6 \times 0.5 \times 0.8$
<i>M</i>	468.61	Transmission: max., min. (%)	1.00, 0.21
<i>a</i> (Å)	14.910(3)	$2\theta(\text{Mo } K\alpha)$ (°)	4–60
<i>b</i> (Å)	0.058(1)	Secondary extinction	$6.0(3) \times 10^{-7}$
<i>c</i> (Å)	18.617(4)	No. measured reflections	2607
β (°)	107.649(8)	No. independent reflections ($I \geq 3(I)$)	1849
<i>V</i> (Å ³)	1602.5(4)	No. variables	148
<i>Z</i>	4	Weight	$1/(\sigma^2(F) + (0.02F)^2 + 1.0)$
Space group	$C2/c$	$R(F_o)$	0.021
D_{calc} (g cm ⁻³)	1.942	$R_w(F_o)$	0.025
$\mu(\text{Mo } K\alpha)$ (cm ⁻¹)	12.7	Goodness of fit	0.49
<i>F</i> (000)	944	Residuals in <i>F</i> map (e Å ⁻³)	–0.54, +0.51

Table 2

Positional parameters and B_{eq}^a (\AA^2) for non-H atoms of $[\text{Rh}(\text{Hdmg})_2(\text{H}_2\text{O})_2]\text{ClO}_4$. The standard uncertainty is reported in parentheses

Atom	x	y	z	B (\AA^2)
Rh	0	0	0	1.453(3)
O1	0.1017(1)	−0.2201(3)	0.14510(8)	2.85(3)
O2	0.0631(1)	0.3969(2)	−0.05555(7)	2.40(2)
O3	0.07900(9)	−0.1812(2)	−0.05005(7)	1.98(2)
N1	0.0999(1)	−0.0464(3)	0.09772(8)	1.89(3)
N2	0.0842(1)	0.2578(3)	0.00197(8)	1.81(2)
C1	0.2509(2)	0.0707(5)	0.1843(2)	3.94(5)
C2	0.1689(1)	0.0920(3)	0.1149(1)	2.16(3)
C3	0.1597(1)	0.2713(3)	0.0597(1)	2.01(3)
C4	0.2322(1)	0.4466(4)	0.0688(1)	2.98(4)
C1	0	−0.2276(2)	−0.25	3.26(1)
O4	0.0668(2)	−0.0910(4)	−0.1966(1)	4.99(4)
O5	0.0470(2)	−0.3586(5)	−0.2907(1)	5.99(5)

^a Anisotropically refined atoms are given in the form of the isotropic equivalent displacement parameter defined as: $(4/3)[a^2B(1,1) + b^2B(2,2) + c^2B(3,3) + ab(\cos \gamma)B(1,2) + ac(\cos \beta)B(1,3) + bc(\cos \alpha)B(2,3)]$.

coefficient was refined in least-squares. The final $R(F_o)$ and $R_w(F_o)$ values are reported in Table 1. Complex neutral-atom scattering factors, including anomalous dispersion terms for all non-H atoms, were taken from International Tables for X-ray Crystallography [14]. Calculations were carried out on a VAX 2000 by using the Molen package [15]. Final non-H positional parameters and B_{eq} (\AA^2) are given in Table 2. See also Section 4.

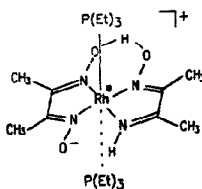
3. Results and discussion

3.1. Synthesis

While attempts to synthesize the $[\text{Rh}(\text{Hdmg})_2(\text{H}_2\text{O})_2]\text{X}$ complexes ($\text{X} = \text{anion}$) from $[\text{Rh}(\text{Hdmg})_2(\text{H}_2\text{dmg})\text{Cl}_2]$, i.e. following the route used for the analogous cobalt derivatives [16], were unsuccessful, **1** could be prepared reacting the Rh(III) hexaqua complex with the stoichiometric amount of dimethylglyoxime in acidic ethanol/water solutions.

Reaction of **1** with two equivalents of PPh_3 , both in acidic and in basic ethanolic solutions, led to the bisphosphine derivative $[\text{Rh}(\text{Hdmg})_2(\text{PPh}_3)_2]\text{ClO}_4$ (**2**). During the reaction an intermediate Rh(II) dimeric species could be envisaged as the solution turned orange–red [12] with strong absorption in the 450 nm region. The species $[\text{Rh}(\text{Hdmg})_2(\text{PPh}_3)_2]^+$ was already reported [4g] as a by-product of the synthesis of $[\text{Rh}(\text{Hdmg})_2\text{ClPPh}_3]$ from $\text{RhCl}_3 \cdot n\text{H}_2\text{O}$, dimethylglyoxime and PPh_3 [17].

The reaction of **1** with PEt_3 following the above procedure did not result in axial water substitution under acidic conditions, while, when carried out in ethanol/water basic solution, it led both to axial substitution and to equatorial ligand reduction giving, after HClO_4 was added, the *trans* bis(triethylphosphine) compound $[\text{Rh}(\text{Hdmg})(\text{Hbdio})(\text{PEt}_3)_2]\text{ClO}_4$ ($\text{Hbdio} = 2,3\text{-butanedione-2-imine-3-oximate}$) (Scheme 1).



Scheme 1. Schematic structure of $[\text{Rh}(\text{Hdmg})(\text{Hbdio})(\text{PEt}_3)_2]\text{ClO}_4$.

The latter species could be identified by NMR since it was already described [7d] as the product of the reaction between $[\text{Rh}(\text{Hdmg})_2(\text{H}_2\text{dmg})\text{Cl}_2]$ and PEt_3 in basic ethanol, both with and without NaBH_4 reduction.

3.2. Crystal structure of $[\text{Rh}(\text{Hdmg})_2(\text{H}_2\text{O})_2]\text{ClO}_4$

An ORTEP [18] drawing with the atom-numbering scheme is shown in Fig. 1. Bond lengths and angles are reported in Table 3. The crystal is built up of $[\text{Rh}(\text{Hdmg})_2(\text{H}_2\text{O})_2]^+$ cations and ClO_4^- anions. The rhodium atom lies on a center of symmetry. The two Hdmg moieties are approximately planar and linked by two intramolecular OHO hydrogen bonds. Bond distances and angles of the equatorial moiety are in agreement with the C_{2h} symmetry already observed [4b] in rhodoximes. In particular the inequality of dimethylglyoximate N–O distances ($\text{N1–O1} = 1.368(2) \text{ \AA}$; $\text{N2–O2} = 1.323(1) \text{ \AA}$) confirms that in the oxime bridges of rhodoximes (O–O distance $2.735(2) \text{ \AA}$) the hydrogen atom is strongly bonded to only one O atom.

The average distance of the Rh–N bonds (1.994 \AA) is slightly longer and that of the CN bonds (1.296 \AA) slightly shorter than the averages of rhodoximes (respectively 1.986 and 1.300 \AA). The Rh–H₂O bond length is $2.031(1) \text{ \AA}$. In the analogous Co complex $[\text{Co}(\text{Hdmg})_2(\text{H}_2\text{O})_2]\text{ClO}_4$ [19], the H₂O coordination distance is 0.13 \AA shorter ($1.900(4) \text{ \AA}$), in agreement with the decrease of the metal ionic radius and the N–metal distance in the equatorial moiety is about 0.09 \AA shorter than in the rhodium complex. The less enhanced difference with respect to the axial H₂O coordination is attributable to the chelation effect.

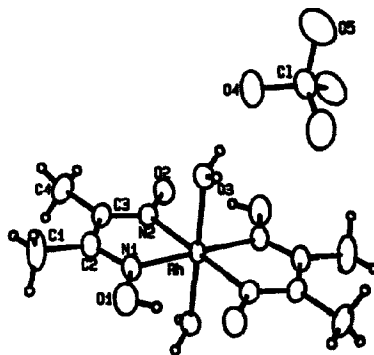


Fig. 1. ORTEP drawing of the compound $[\text{Rh}(\text{Hdmg})_2(\text{H}_2\text{O})_2]\text{ClO}_4$.

Table 3

Selected bond lengths (Å) and angles (°) for $[\text{Rh}(\text{Hdmg})_2(\text{H}_2\text{O})_2]\text{ClO}_4$ with e.s.d.s in parentheses

Rh O3	2.031(1)	O1 N1	1.368(2)	N2 C3	1.302(2)	C3 C4	1.487(3)
Rh N1	1.991(1)	O2 N2	1.324(2)	C1 C2	1.491(3)	Cl O4	1.437(2)
Rh N2	1.998(2)	N1 C2	1.290(2)	C2 C3	1.473(3)	Cl O5	1.420(3)
O3 Rh N1	88.02(6)	Rh N2 C3	116.5(1)	N2 C3 C4	123.7(2)		
O3 Rh N2	88.98(6)	O2 N2 C3	124.2(2)	C2 C3 C4	122.5(1)		
N1 Rh N2	78.56(6)	N1 C2 C1	122.7(2)	O4 Cl O4	109.7(1)		
Rh N1 O1	124.1(1)	N1 C2 C3	114.1(1)	O4 Cl O5	109.9(1)		
Rh N1 C2	117.0(1)	C1 C2 C3	123.2(2)	O4 Cl O5	107.7(1)		
O1 N1 C2	118.8(1)	N2 C3 C2	113.8(2)	O5 Cl O5	112.1(2)		
Rh N2 O2	119.3(1)						

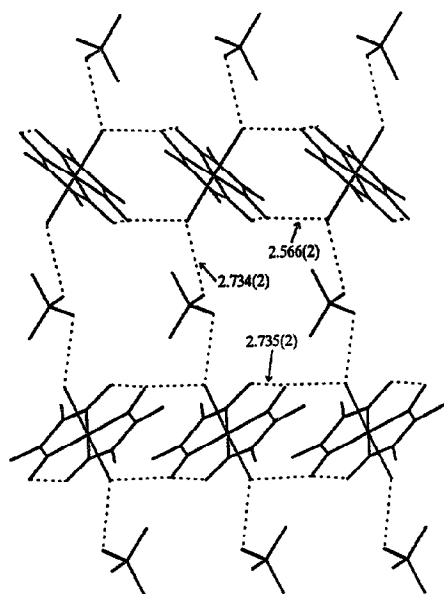


Fig. 2. Inter- and intramolecular hydrogen bonding scheme.

An interesting feature is that the coordinated water molecule is involved in two hydrogen bonds, one with an oxime O atom of another cation and the other with an O atom of the

perchlorate anion (Fig. 2). The hydrogen bond that links the cations together is particularly strong, the O...O distance being 2.566(2) Å. This can also account for the very long OH...O distance.

3.3. IR spectra

For the rhodoximes of Table 4 the absorptions in the range 1518–1535 cm^{-1} are due mainly to C–N stretching [20], and occur at lower frequencies than for the corresponding cobaloximes [21]. The $[\text{Rh}(\text{Hdmg})(\text{H}_2\text{dmg})\text{Cl}_2]$ derivative, which has one of the equatorial hydrogen bridges broken due to protonation, shows much higher νCN (1596 cm^{-1}). Thus the value found for $[\text{Rh}(\text{Hdmg})_2(\text{H}_2\text{O})_2]\text{ClO}_4$ (1535 cm^{-1}) reflects intact proton bridges, in agreement with the symmetry and the O–O distances of the X-ray structure. The registered C–N frequencies decrease in the order $[\text{Rh}(\text{Hdmg})_2(\text{H}_2\text{O})_2]\text{ClO}_4 > [\text{Rh}(\text{Hdmg})_2(\text{PPh}_3)\text{Cl}] > [\text{Rh}(\text{Hdmg})_2(\text{PPh}_3)_2](\text{ClO}_4)$, while the C–N distances are 1.2962(2), 1.292(7) [4h] and 1.290(7) Å [22], respectively.

This is in line with that these vibrations are not pure C–N stretches [20] and could be due to the expected weakening of the back donation from the metal towards the equatorial ligand when two water molecules are in axial positions, as well as to the effect of the intermolecular hydrogen bonds on the equatorial oxygen's electron density. These findings and

Table 4

Selected IR data for some rhodoximes

Compound	ν (cm^{-1})				
	C–N	N–O	Rh–N	Rh–Cl	ClO_4
$[\text{Rh}(\text{Hdmg})(\text{H}_2\text{dmg})\text{Cl}_2] \cdot 5\text{H}_2\text{O}$	1596m	1240vs 1070vs	510s	370m	
$[\text{Rh}(\text{Hdmg})_2(\text{H}_2\text{O})_2]\text{ClO}_4$	1535s	1246vs 1085vs 1255vs 1092vs	512s		629
$[\text{Rh}(\text{Hdmg})_2(\text{Cl})(\text{PPh}_3)]$	1530vs	1260vs 1072s	514s	350m	
$[\text{Rh}(\text{Hdmg})_2(\text{PPh}_3)_2]\text{ClO}_4 \cdot \text{H}_2\text{O}$	1518s	1260s 1090vs	520s		622

the known dependence of ν_{CN} on the counterion M^+ , reported for a series of $[\text{Co}(\text{Hdmg})_2(\text{NO}_2)_2]M$ complexes [23], show that the interpretation of such data requires great care.

3.4. NMR spectra

The Rh(III) rhodoximes are scarcely prone toward axial substitution. Even in organorhodoximes $[\text{RRh}(\text{Hdmg})_2\text{L}]$ the exchange of L is slow and usually no coalescence of the signals is observed [24] notwithstanding the strong *trans* effect of the alkyl. When the *trans* effect is smaller the substitutions are much slower [1c]. As only one species is detected by NMR spectra in the freshly prepared DMSO- d_6 solutions of 1, this species must be 1 itself. The same holds for 2.

The NMR spectra of 2 confirm the previous findings about the apical *trans* influence. The $^1J(\text{P},\text{C})$ value provided by the ^{13}C spectra can be considered a measure of the involvement of the phosphorus lone pair in binding the metal [25]; in triphenylphosphine rhodoximes $^1J(\text{P},\text{C})$ increases as the ligand *trans* to phosphorus changes from methyl [24] to PPh_3 , to Cl [4g], to H_2O [4g], (30, about 47, 53 and 59 Hz,

respectively). For the bisphosphine derivative 2 the value cannot be obtained directly from the spectrum, the overall splitting corresponding to $^1J(\text{P},\text{C}) + ^3J(\text{P}',\text{C})$. However rhodoximes with a trialkylphosphine in *trans* to PPh_3 show $^3J(\text{P}',\text{C})$ of a few Hz [24] and this allows the value reported above for $^1J(\text{P},\text{C})$ to be estimated. The same trend is found for the $^1J(\text{Rh},\text{P})$ coupling constant, which is a recognized indicator of the *trans* influence [4g,1b].

The spectra of 1 and 2 could provide information on the behavior of the equatorial macrocycle in rhodoximes, which needs better understanding. Indeed its bond lengths and angles show just small variations and the interpretation of the changes in its IR spectra is not straightforward.

Inspection of the glyoximate methyl proton shifts shows that the compounds of Table 5 can be divided into three groups: no PPh_3 (δ 2.36–2.47 ppm), one PPh_3 (δ 1.74–1.94 ppm), two PPh_3 (δ 1.38–1.48 ppm); the shielding increases with the number of phosphine phenyls, their magnetic anisotropy being the major factor in determining these chemical shift differences.

The equatorial carbon shows notable shift variations, Table 6. For 1 they are deshielded with respect to the methylaqua $[\text{CH}_3\text{Rh}(\text{Hdmg})_2\text{H}_2\text{O}]$ derivative [24] both in

Table 5
Selected ^1H NMR spectral data for rhodoximes, δ (ppm)

Compound	Solvent	PPh_3	Hdmg
$[\text{Rh}(\text{Hdmg})(\text{H}_2\text{dmg})\text{Cl}_2]$	DMSO- d_6		2.36 s
$[\text{Rh}(\text{Hdmg})_2(\text{H}_2\text{O})_2]\text{ClO}_4$	DMSO- d_6		2.37
	D_2O		2.47 s
	CDCl_3		2.36 s
$[\text{Rh}(\text{Hdmg})_2\text{Cl}(\text{PPh}_3)]^a$	CDCl_3	7.49–7.41 m	1.94 d (0.5) ^a
	CD_3OD	7.43–7.22 m	1.74
$[\text{Rh}(\text{Hdmg})_2(\text{PPh}_3)_2]\text{ClO}_4$	DMSO- d_6	7.57–7.39 m	1.38 t (1.5) ^a
	CDCl_3	7.58–7.36 m	1.48 t (1.5) ^a

^a $^5J(\text{P},\text{H})$ in Hz.

^b See Ref. [4g].

Table 6
 ^{13}C and ^{31}P NMR data for rhodoximes, δ (ppm)

Compound	Solvent	Phosphine				
		^{31}P	C-1	C-2	C-3	C-4
$[\text{Rh}(\text{Hdmg})(\text{H}_2\text{dmg})\text{Cl}_2] \cdot 5\text{H}_2\text{O}$	DMSO- d_6					
$[\text{Rh}(\text{Hdmg})_2(\text{H}_2\text{O})_2]\text{ClO}_4$	DMSO- d_6					
	D_2O					
$[\text{Rh}(\text{Hdmg})_2\text{Cl}(\text{PPh}_3)]^d$	CDCl_3	23.8 (123) ^a	127.0 (53) ^b	134.0 (10) ^b	128.4 (10) ^b	131.6 (3) ^b
$[\text{Rh}(\text{Hdmg})_2(\text{PPh}_3)_2]\text{ClO}_4 \cdot \text{H}_2\text{O}$	DMSO- d_6	17.3 (91) ^a	127.5 (50) ^c	135.3	130.4	133.4
	CDCl_3	16.7 (91) ^a	125.9 (50) ^c	133.9	128.9	132.2

^a $^1J(\text{Rh},\text{P})$ in Hz.

^b $^1J(\text{P},\text{C})$ in Hz.

^c $^1J(\text{P},\text{C}) + ^3J(\text{P}',\text{C})$ in Hz.

^d See Ref. [4g].

DMSO- d_6 and D_2O solutions (about 3 ppm for CN and about 1 ppm for CH_3). For **2** they are deshielded with respect to $[CH_3Rh(Hdmg)_2PPh_3]$ and $[ClRh(Hdmg)_2PPh_3]$ in $CDCl_3$ (about 5 and about 4 ppm, respectively, for CN, and about 0.5 ppm for CH_3).

For $[Rh(Hdmg)_2(H_2O)(PPh_3)]^+ [4g]$ they are deshielded with respect to $[CH_3Rh(Hdmg)_2PPh_3]$ [**24**] in acetone- d_6 (5.6 ppm for CN and 0.6 ppm for CH_3). **1** and **2** in DMSO have almost identical CN shifts, while the equatorial methyl of the latter is about 2 ppm more shielded, partially due to the phosphine phenyls. Thus it can be inferred that the electric charge of the complex affects strongly the resonance of the CN carbon, which is notably deshielded in the cationic rhodoximes.

3.5. Electrochemistry of $[Rh(Hdmg)_2(PPh_3)_2]ClO_4$

Electrochemical data of rhodoximes are very scarce (Table 7) [5b,c]. The signals are often very difficult to explain and the change of electrode materials (Pt, Au, glassy carbon) and solvents (DMSO, acetonitrile) does not help much. This happens also with $[Rh(Hdmg)_2(H_2O)_2]ClO_4$. On the contrary $[Rh(III)(Hdmg)_2(PPh_3)_2]ClO_4$ gave good electrochemical results.

The polarography in DMF in the range from +0.4 to -2.7 V shows three equally high monoelectronic reduction waves. The first one at -0.60 V, assigned to the reduction $Rh(III)/Rh(II)$, is electrochemically quasi-reversible and followed by a maximum attributed to adsorption phenomena; the second one at -1.47 V, assigned to the reduction $Rh(II)/Rh(I)$, is electrochemically reversible; the third one at -2.06 V is also reversible but it is not attributed at the moment. The linear increase of the limiting currents with concentration up to 1.5 mmol shows the diffusion character of all these signals.

The cyclic voltammetry on Hg electrode at scan rate of $1 V s^{-1}$ (Fig. 3) shows three cathodic monoelectronic peaks: $E_{pc}(III)/(II) = -0.68 V$, strongly disturbed by a series of adsorption peaks; $E_{pc}(II)/(I) = -1.555 V$; $E_{pc}' = -2.091 V$, with a small adsorption signal. The electron transfers (ET) corresponding to the first two peaks are followed by fast chemical reactions as they show no anodic counterpart up to a scan rate of $1000 V s^{-1}$ [26].

About the $Rh(III)/Rh(II)$ reactions it is noteworthy that:

(i) for $[Rh(Hdmg)(Hbdio)(PEt_3)_2]$ this reduction potential [7d] is much more negative than for $[Rh(Hdmg)_2(PPh_3)_2]ClO_4$, possibly due to the combined effects of the

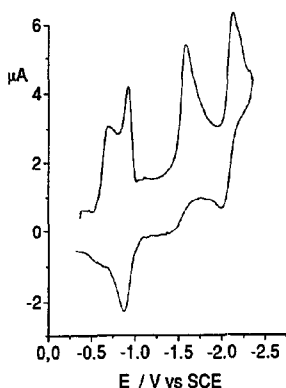


Fig. 3. Cyclic voltammetry of the compound $[Rh(Hdmg)_2(PPh_3)_2]ClO_4$ in DMF + TBAP 0.1 M at 25°C on Hg electrode at $1 V s^{-1}$.

greater basicity of PEt_3 and of the $(Hdmg)(Hbdio)$ equatorial ligand;

(ii) for $[Rh(Hdmg)_2PPh_3Cl]$ this reduction potential is much more negative than for $[Rh(Hdmg)_2(PPh_3)_2]ClO_4$. Perhaps this reflects a noticeably higher electron density at rhodium when a chloride replaces one PPh_3 , and is in relation with the above reported higher shielding of the CN carbon observed in the neutral chloro complex.

The CV signals show that the ET of this reduction is monoelectronic and is always followed by a fast chemical reaction: for $[Rh(Hdmg)_2PPh_3Cl]$ [5c] and $[Rh(Hbdio)(Hdmg)-(PEt_3)_2]ClO_4$ [7d] it was shown that the product of this following coupled reaction is the formation of an $Rh(II)$ dimer.

4. Supplementary material

H atom coordinates, anisotropic thermal parameters, and a list of calculated and observed structure factors are available from the authors on request.

Acknowledgements

This work was supported by the Consiglio Nazionale delle Ricerche (CNR, Rome, Italy) and by the Ministero dell'Università e delle Ricerche Scientifica e Tecnologica (40% and 60% MURST, Rome, Italy). M.M. acknowledges the Consorzio per lo sviluppo Internazionale dell'Università di Trieste for a fellowship.

References

- (a) M. Kubiak, T. Glowiak, M. Moszner, J.J. Ziolkowski, F. Asaro, G. Costa, G. Pellizer and C. Tavagnacco, *Inorg. Chim. Acta*, **236** (1995) 141; (b) M. Ludwig, L. Öhrström and D. Steinborn, *Magn. Reson. Chem.*, **33** (1995) 984; (c) C. Dückner-Benfer, R. Drees and

Table 7
Electrochemical data for the first ET of some rhodoximes in DMF + TEAP 0.1 M at 25°C

Complex	$E_{1/2}$ (V)	Ref.
$[Rh(III)(Hdmg)_2(PPh_3)_2]^+$	-0.60	
$[Rh(III)(Hdmg)(H_2dmg)Cl_2]$	-0.75	
$[Rh(III)(Hdmg)_2Cl(PPh_3)_2]$	-1.010	[5c]
$[Rh(Hdmg)(Hbdio)(PEt_3)_2]$	-1.25	[7d]

- R. van Eldik, *Angew. Chem., Int. Ed. Engl.*, **34** (1995) 2245; (d) M. Dunaj-Jurco, D. Miklos, I. Potocnak, M. Ludwig and D. Steinborn, *Acta Crystallogr., Sect. C*, **52** (1996) 315; (e) F. Asaro, G. Costa, R. Dreos, G. Pellizer and W.v. Philipsborn, *J. Organomet. Chem.*, **513** (1996) 193.
- [2] (a) E.N. Sainikova and M.L. Khidekel, *Izv. Akad. Nauk. SSSR, Ser. Khim.*, (1967) 223; (b) W.B. Panov, M.L. Khidekel and S.A. Shchepimov, *Izv. Akad. Nauk. SSSR, Ser. Khim.*, (1968) 239; (c) B.T. Rogachev and M.L. Khidekel, *Izv. Akad. Nauk. SSSR, Ser. Khim.*, (1969) 141; (d) K.R. Howes, A. Bakac and J.H. Espenson, *Inorg. Chem.*, **27** (1988) 3147; (e) D. Steinborn, U. Sedlak and M. Dargatz, *J. Organomet. Chem.*, **415** (1991) 407.
- [3] (a) N. Bresciani-Pahor, M. Forcolin, L.G. Marzilli, L. Randaccio, M.F. Summers and P.J. Toscano, *Coord. Chem. Rev.*, **63** (1985) 1; (b) C. Tavagnacco, G. Balducci, G. Costa, K. Täschler and W.v. Philipsborn, *Helv. Chim. Acta*, **73** (1990) 1469.
- [4] (a) N. Bresciani-Pahor, R. Dreos-Garlatti, S. Geremia, L. Randaccio, G. Tauzher and E. Zangrando, *Inorg. Chem.*, **29** (1990) 3437; (b) L. Randaccio, S. Geremia, R. Dreos-Garlatti, G. Tauzher, F. Asaro and G. Pellizer, *Inorg. Chim. Acta*, **194** (1992) 1; (c) S. Geremia, R. Dreos, L. Randaccio and G. Tauzher, *Inorg. Chim. Acta*, **216** (1994) 125; (d) C. Bied-Charreton, A. Gaudemer, C.A. Chapman, D. Dodd, B. Dass Gupta, M.D. Johnson, B.L. Lockman and B. Septe, *J. Chem. Soc., Dalton Trans.*, (1978) 1807; (e) B. Giese, J. Hartung, C. Kesselheim, H.J. Lindner and I. Svoboda, *Chem. Ber.*, **126** (1993) 1193; (f) D. Steinborn and M. Ludwig, *J. Organomet. Chem.*, **463** (1993) 65; (g) F. Asaro, R. Dreos-Garlatti, G. Pellizer and G. Tauzher, *Inorg. Chim. Acta*, **211** (1993) 27; (h) F.A. Cotton and J.G. Norman, Jr., *J. Am. Chem. Soc.*, **93** (1971) 80.
- [5] (a) G. Costa, A. Puxeddu, C. Tavagnacco, G. Balducci and R. Kumar, *Gazz. Chim. Ital.*, **116** (1986) 735; (b) M.V. Kljuev, M.L. Khidekel' and V.V. Strelets, *Transition Met. Chem.*, **3** (1978) 380; (c) C. Tavagnacco et al., manuscript in preparation.
- [6] F.P. Dwyer and R.S. Nyholm, *Proc. R. Soc. N.S.W.*, **78** (1944) 266.
- [7] (a) Yu.A. Simonov, T.V. Timofeeva, A.A. Dvorkin, Yu.T. Struchov, I.A. Nemchinova and O.A. Bologa, *Koord. Khim.*, **7** (1981) 428; (b) Yu.A. Simonov, L.A. Nemchinova, A.V. Ablov, V.E. Zavodnik and O.A. Bologa, *Zh. Strukt. Khim.*, **17** (1976) 142; (c) Yu.A. Simonov, L.A. Nemchinova and O.A. Bologa, *Kristallografiya*, **24** (1979) 829; (d) R. Dreos, G. Tauzher, S. Geremia, L. Randaccio, F. Asaro, G. Pellizer, C. Tavagnacco and G. Costa, *Inorg. Chem.*, **33** (1994) 5404.
- [8] Yu.A. Simonov, A.A. Dvorkin, L.A. Nemchinova, O.A. Bologa and T.I. Malinowskii, *Koord. Khim.*, **7** (1981) 125.
- [9] A.V. Ablov, L.A. Nemchinova, M.P. Filippov and O.A. Bologa, *Zh. Neorg. Khim.*, **22** (1977) 425.
- [10] G.H. Ayres and J.S. Forrester, *J. Inorg. Nucl. Chem.*, **3** (1957) 365.
- [11] D. Britz, *Electrochim. Acta*, **25** (1980) 1449.
- [12] T. Ramasami and J.H. Espenson, *Inorg. Chem.*, **19** (1980) 1846.
- [13] W.H. Zachariasen, *Acta Crystallogr.*, **16** (1963) 1139.
- [14] *International Tables for X-ray Crystallography*, Vol. IV, Kynoch, Birmingham, UK, 1974.
- [15] B.A. Frenz, The Enraf-Nonius CAD4 SDP, a real-time system for concurrent X-ray data collection and crystal structure determination, in H. Schenk, R. Olthof-Hazekamp, H. van Koningsveld and G.C. Bassi (eds.), *Computing in Crystallography*, Delft University Press, Delft, Netherlands, 1978.
- [16] A.V. Ablov and N.M. Samus', *Russ. J. Inorg. Chem.*, (1960) 5.
- [17] P. Powell, *J. Chem. Soc. A*, (1969) 2418.
- [18] Jonson, *ORTEP*.
- [19] M. Pyckhout, A.T.H. Lenstra and S.K. Tyrtik, *Bull. Soc. Chim. Belg.*, **96** (1987) 575.
- [20] (a) R. Blinc and D. Hadzi, *J. Chem. Soc.*, (1958) 4536; (b) R.S. Drago and J.H. Elias, *J. Am. Chem. Soc.*, **90** (1977) 6570; (c) G. Wilkinson, R.D. Gillard and J.A. McCleverty, *Comprehensive Coordination Chemistry*, Vol. 2, Pergamon, Oxford, 1987.
- [21] H.A.O. Hill and K.G. Morallee, *J. Chem. Soc. A*, (1969) 554.
- [22] M. Moszner, M. Kubiak, T. Głowiak and J.J. Ziolkowski, to be published.
- [23] N. Yoshida, A. Furusaki and M. Fujimoto, *J. Chem. Soc., Dalton Trans.*, (1991) 453.
- [24] E. Del Frari, F. Asaro and G. Pellizer, unpublished results.
- [25] V.M.S. Gil and W.v. Philipsborn, *Magn. Reson. Chem.*, **27** (1989) 409.
- [26] R.W. Rossiter and I.F. Hamilton (eds.), *Physical Methods of Chemistry, Electrochemical Methods*, Vol. II, Wiley, New York, 1985.